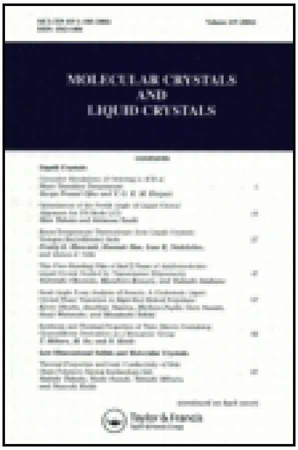

Molecular Crystals and Liquid Crystals Incorporating Nonlinear Optics

Publication details, including instructions for authors and subscription information:
http://www.tandfonline.com/loi/gmcl17

Liquid Crystalline Catalysis by Smectic B Solvents: Structure and Thermodynamical Properties of the Reactant Solution

G. Albertini [a] , P. Mariani [a] , F. Rustichelli [a] & B. Samori [b]

[a] Facoltà di Medicina e Chirurgia, Università di Ancona, via Monte d'Ago, 60100, Ancona, Italy

[b] Università di Bologna, via Risorgimento 4, 40136, Bologna, Italy

Version of record first published: 03 Jan 2007.

To cite this article: G. Albertini , P. Mariani , F. Rustichelli & B. Samori (1988): Liquid Crystalline Catalysis by Smectic B Solvents: Structure and Thermodynamical Properties of the Reactant Solution, Molecular Crystals and Liquid Crystals Incorporating Nonlinear Optics, 163:1, 163-176

To link to this article: http://dx.doi.org/10.1080/00268948808081996

Mol. Cryst. Liq. Cryst., 1988, Vol. 163, pp. 163–176
Reprints available directly from the publisher
Photocopying permitted by license only

Printed in the United States of America

Liquid Crystalline Catalysis by Smectic B Solvents: Structure and Thermodynamical Properties of the Reactant Solution

G. ALBERTINI, P. MARIANI and F. RUSTICHELLI
Facoltà di Medicina e Chirurgia, Università di Ancona, via Monte d'Ago, 60100 Ancona, Italy

and

B. SAMORI
Università di Bologna, via Risorgimento 4, 40136 Bologna, Italy

(*Received June 18, 1987; in final form January 2, 1988*)

ASE quaternization reaction was used as a reactivity probe within smectic B solvents. The aim of the present study is to point out the determinant role that differential scanning calorimetry (DSC) and x-ray scattering techniques may play within this kind of investigation. DSC is proving to be particularly valuable to display the multisite distribution of a solute molecule within the smectic B solution. The reactant partition between different sites, previously suggested also on the basis of linear dicroism spectra, is particularly important because it provides a unifying framework able to account for all the reactivity and structural experimental data previously published by us.

Keywords: liquid crystalline catalysis, smectic B solvent

1. INTRODUCTION

The first investigations searching the possible influences of thermotropic liquid–crystalline solvents on the rates and stereochemistry of thermal reactions were rather discouraging.[1-5]

We know, now, that the main reason of these frustrating initial results was the use of solvents in their nematic or cholesteric phase.

In fact in these liquid-crystalline phases the "microscopic matrix effect," exerted by the short-range orientational order, is not very different from that of isotropic solvents.[6] We thus managed to use smectic B phases as catalytic solvents because of our feeling that only more tightly ordered mesophases could provide anisotropic constraints to the conformation and diffusion properties of solute reactant molecules, strong enough to significantly decrease or increase reaction free energies of activation.

We have thus been searching for liquid-crystalline catalysis effects by using several mesomorphic compounds: ZLI-1409,[7,8] ZLI-1544,[7,9] ZLI-1756,[10] OS-44,[11] OS-53,[11] OS-35.[11,12] The influence of these smectic B solvents on monomolecular or bimolecular reactions was observed by using as reactivity probes the monomolecular rearrangements of limonene or linallol[9] and the bimolecular quaternization of methyl- and allyl-*p*-(dimethyl-amino) benzen sulfonate (MSE or ASE, respectively).[7,8,10-12] The ASE quaternization is represented here.

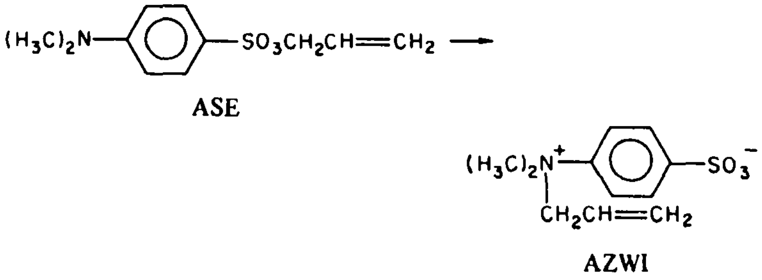

CHART 1

After our first positive results, smectic B media have been checked as solvents for very different kinds of reactions also by other scientists and some very promising results have been obtained.[13-15] By enlarging the number of physical techniques used within our investigations, we have been furthering our knowledge of this catalytic process. Very recently we have also carried out polymerization of bisacrylic monomers in smectic B solvent[16] and asymmetric inductions within chiral smectic C* and smectic A* solvents.[17] Smectic B mesophases therefore appeared to provide a very good compromise between the reactivity in solid and in liquid media: in fact they are able to supply very anisotropic potentials to molecular orientations[18,19] as the solid phases can, while the limitation due to low diffusion in solids does not occur.

In order to achieve a better understanding at molecular level of the catalytic effect, a detailed knowledge of the reactant-solvent mixture within the "reaction pot" is required. Within the investigation of the ASE quaternization reaction in OS-35 liquid crystal, differential scanning calorimetry (DSC), optical microscopy (OM), x-ray diffraction, kinetic measurements and linear dichroism (LD) were recently used to this purpose.[12] This paper reports the significant progress made in the DSC analysis of these reactive solutions. A different mesomorphic solvent (ZLI-1409) was used, the smectic and nematic phases of which exist in a larger range of temperature with respect to OS-35, so that the coexistence of phases is more easily avoidable and a better resolution of the DSC peaks is achieved.

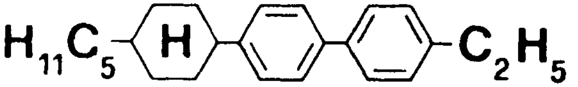

ZLI 1409

CHART 2

2. MATERIALS AND METHODS

The synthesis of ASE was carried out according to the procedure used in Ref. 12. ASE was dissolved in the ZLI-1409 solvent at room temperature by injections of volumes of a diethyl ether solution of known concentration: after complete evaporation under vacuum of all the volatile solvent traces, the homogeneous solutions of ASE were partitioned and analysed by different techniques.

The DSC measurements were carried out on a Perkin Elmer Calorimeter Model DSC-2c with related data processor. The usual scan rate was 2.5 °C/min both on heating and on cooling processes. Aluminum containers of 20 μl capacity were used.

Optical microscopy was performed with a polarizing microscope (Leitz Ortolux 2 Pol) equipped with a Mettler FP 52 hot-stage. Scan rates of 1°C/min were used during the heating and of 0.2°C/min during the cooling.

In x-ray diffraction experiments, goniometric scans were obtained by using a conventional powder diffractometer. Ni-filtered Cu-Kα radiation (λ = 1.54 Å) was used. The divergence of the primary beam impinging on the sample was ≈8′. The generator-sample distance was 18 cm and the sample counter distance was 20 cm. The sample had thickness of ≈1.5 mm and was sandwiched between two very thin aluminum sheets fixed to a circular hole in an aluminum matrix with diameter of ≈1 cm. Heating was obtained by a hot stage containing electrical resistors, the temperature of which was controlled to 0.1°C by a BT 300/301 control system supplied by SMC, Grenoble (France).

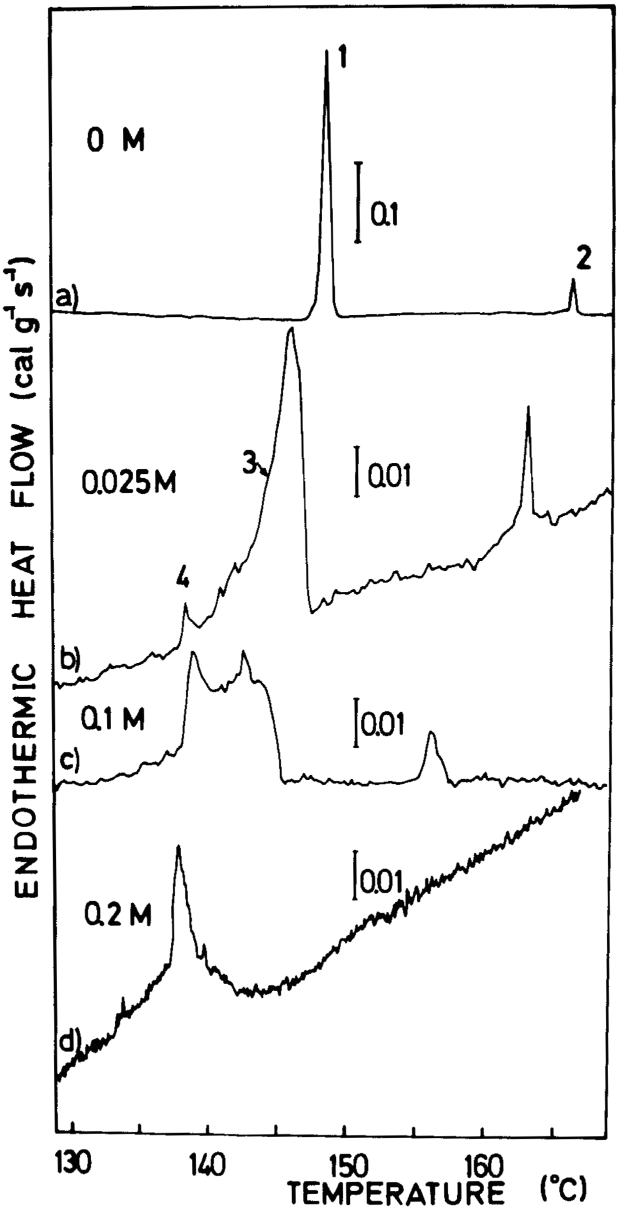

FIGURE 1 Calorimetric scans obtained from pure ZLI-1409 (a) and 0.025 M (b), 0.1 M (c) and 0.2 M (d) ASE in ZLI-1409 (Scan rate = 2.5°C/min).

3. RESULTS

3.1. Calorimetry

Some DSC thermograms, obtained on heating mixtures with different ASE concentrations, are reported in Figure 1. The first, (a), is that of the pure solvent and shows the two peaks labelled "1" and "2" relative to the transitions from smectic B to nematic and from nematic to isotropic phases, respectively.

On increasing the reactant concentration, the temperature of the two transitions gradually lower and their peaks broaden. Several very small signals start appearing already at the lowest ASE concentrations. In particular, a shoulder, labelled "3" in Figure 1, arises on low temperature side of peak "1". At ASE concentration greater than $1 * 10^{-2}$ M, the DSC profile exhibits a new peak ("4") which grows in area at the expense of the parent peak ("1" + "3") as the guest concentration increases.

The calorimetric patterns gradually change along successive cooling and heating cycles. Only calorimetric data obtained in the first heating scan are thus presented and discussed in this paper.

Figure 2 reports the temperatures corresponding to the maxima of "1", "2" and "4" peaks detected in the first calorimetric heating scan, together with the inferred position of the shoulder "3", as a function of ASE molar concentration. The so obtained phase diagram indicates that the two-component system gives rise to an eutectic (having a transition temperature of ≈138°C – peak "4") for high ASE concentration.

Enthalpy variation at the smectic to nematic phase transition is shown in Figure 3 as a function of ASE content. A decrease in enthalpy is evident until the peak disappears for concentration greater than 0.1 M.

It is noteworthy that a very similar calorimetric behavior was observed in the case both of ASE and OS-35 binary mixture[12] and of the reaction mixture of bisacrylic monomers and OS-35.[16] This fact will be considered in the discussion.

3.2. Optical Microscopy

Optical microscopy showed that the solution is nematic between calorimetric peaks "1" and "2" and smectic below peak "1". The smectic B texture remained unchanged at different temperatures for mixtures at very low ASE concentration. On the other hand, changes in

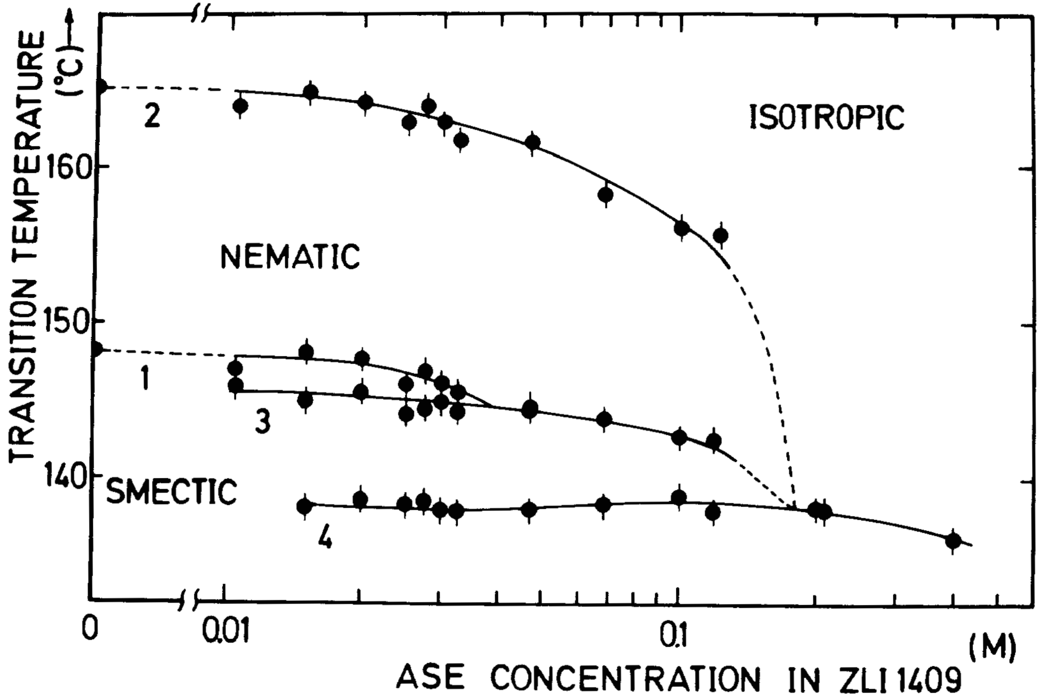

FIGURE 2 Transition temperatures, as obtained from calorimetric peak maxima (see text), as a function of ASE molar concentration in ZLI-1409. The numbers refer to the peaks reported in Figure 1.

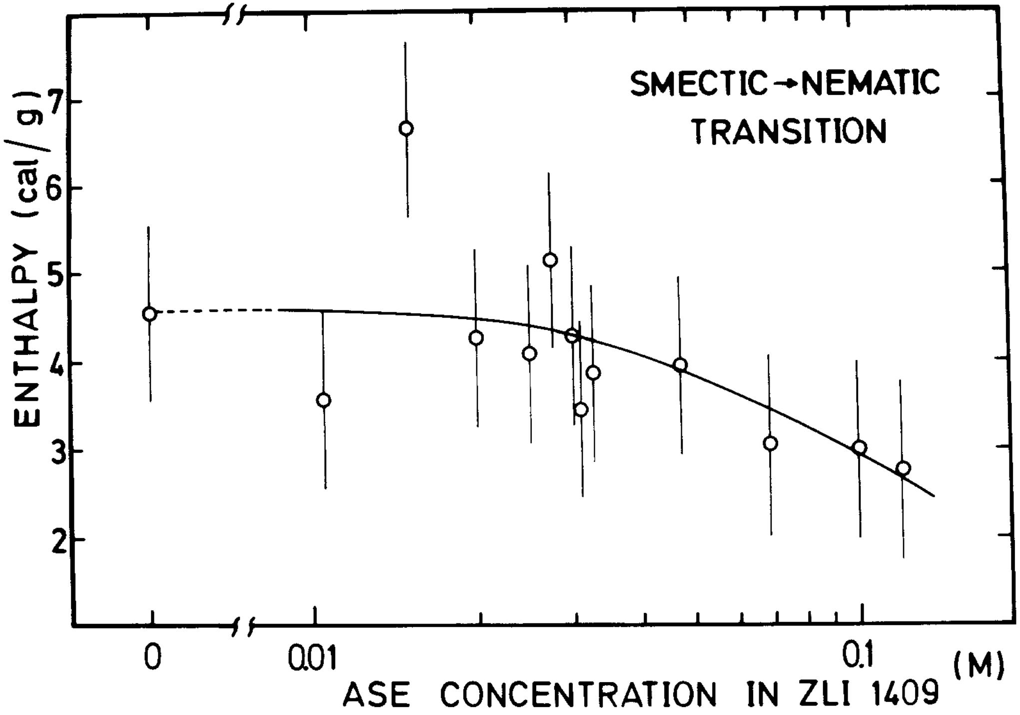

FIGURE 3 Total enthalpy at the smectic–nematic transition as a function of ASE molar concentration in ZLI-1409.

the texture were observed at higher solute concentration (still below 0.1 M) on crossing the eutectic transition temperature: in addition the overall smectic B mosaic organization appears to be in equilibrium with both isotropic and nematic phases. Finally, at the highest concentrations a transition from smectic B to isotropic phase appears at ≈137°C.

The coexistence of the three phases, which is forbidden by the Gibbs phase rule, is not very surprising. In fact the phase rule was established for the melting of a perfect infinite crystal where all the molecules are forced together to cooperate in the transition.[20] In our binary case the cooperative unit (*i.e.* the number of molecules which cooperate) will be smaller than the whole bulk owing to local structural imperfections and non-ideal mixing of the two components. Therefore, in these cases the Gibbs phase rule cannot be strictly applied and phase diagrams cannot be rigorously constructed. For this reason, Figure 2 only reports the mid-points of the transitions, which may thus be considered as the phase transition temperature.

3.3. X-Ray Diffraction

The x-ray diffraction profiles showed by ZLI-1409-ASE mixtures are basically the same as those reported in reference 8 for the pure solvent. The interlayer and the intermolecular distances, which can be derived from the low- and high-angle peaks respectively, are not significantly affected by the ASE presence.

As an example, Table I reports the intermolecular distance d obtained in the smectic B phase at 40°C for various ASE concentrations and the corresponding coefficients of thermal dependence. This last value is the angular coefficient of the best-fit straight line drawn by considering a linear dependence of d with respect to temperature.

TABLE I

Intermolecular distance d at 40°C and its temperature dependence

ASE concentration (mM)	d(Å) (T = 40°C) (± 0.01 Å)	d/t (Å/°C) × 10^3 (± 0.04 * 10^{-3} Å/°C)
10.5	5.39	0.99
46.8	5.38	1.01
47.0	5.38	1.01
68.2	5.38	0.98
68.7	5.38	0.96
119.0	5.39	0.94
123.0	5.38	0.96
208.0	5.38	0.94

Variations are just at the limits of the experimental error. However it should be pointed out that these coefficients reported in the last column seem to decrease for increasing ASE concentration.

Also the width of the diffraction peaks does not vary appreciably with ASE concentration. In particular Figure 4 reports the low angle and high angle peaks obtained at 40°C from a sample with 0.2 M ASE concentration. The width of the peaks, which is larger for shorter range of correlation, appears to be as small as it is for pure ZLI-1409 in the same smectic B phase, indicating a strong long-range order.

4. DISCUSSION

The behavior observed in ZLI-1409 and ASE mixtures appears to be quite general: in fact a similar phase diagram was observed also by using a different liquid cristalline solvent, namely OS-35, both with the same reactant[12] and with bisacrylate monomer.[16] Moreover, in all the investigated cases, x-ray diffraction experiments showed that the catalytic smectic B phase exists even at high solute concentration without detectable structural modifications.

On the other hand, the calorimetric profiles obtained at different solute concentration undergo significant changes in shape, which are similar for all the binary mixtures we have studied so far. Moreover, the discontinuities observed in the kinetic patterns of the ASE reaction[12] and some reactivity data of MSE rearrangement[7,8] indicate that local changes do exist inside the unperturbed smectic B phase.

The DSC behavior may be analyzed by using the same approach used to interpret thermograms of phospholipid bilayers containing small molecules.[21] The effect of over one hundred hydrophobic solute molecules on the gel to liquid crystalline phase transition patterns of synthetic phosphatidyl-cholines were studied by DSC: at least four different types of modified transition profiles were distinguished.

In so-called type C profiles the guest molecules cause a shift of the transition temperature (Tm) usually (but not always) towards lower temperatures, while having little or no effect on enthalpy (H) variation and on the half-height-width (HHW) of the transition peak, *i.e.* on the cooperativity of the transition.[22] Additives producing this behavior seem to be localized in the central region of the bilayer.

Type A profiles, which are due to guest partially buried in the hydrocarbon core of the bilayer, are characterized by a shift in Tm, usually to a lower temperature, and by an increase in HHW while H is practically unaffected.

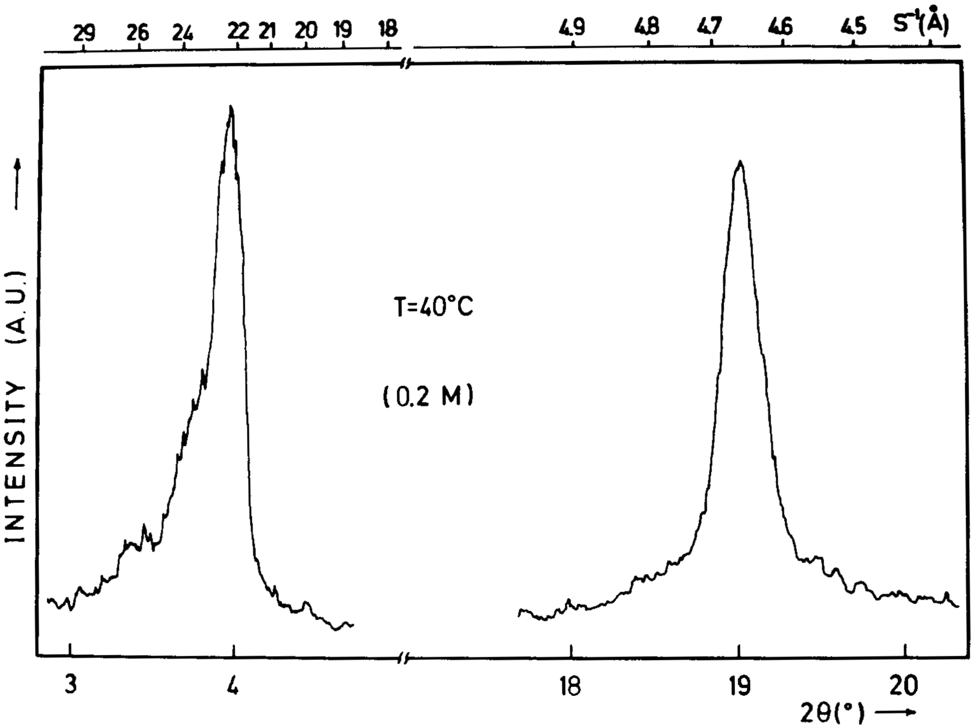

FIGURE 4 X-ray diffraction patterns obtained from a mixture of 0.2 M ASE in ZLI-1409 at T = 40°C. X-ray diffracted intensity is reported as a function of scattering angle 2θ. The S^{-1} units are also reported, being $S = 2 \sin\theta/\lambda$.

In type B profiles a shoulder emerges and grows with the additive concentration at the expense of the main transition peak. The total shoulder-peak area remains unchanged, at least at low additive concentration. Additives which produce type B profiles are generally localized at the hydrophobic–hydrophilic interface of the bilayer and primarily interact with the glycerol backbone of the phospholipid molecules.

Finally, type D profiles exhibit a discrete new peak which grows in area at the expense of the parent peak as the additive concentration increases. Type D additives seem to be located at the bilayer surface and to mainly interact with the phosphorylcholine headgroup.

The phospholipid bilayers are lyotropic smectic liquid crystals. Their chemical constitution is totally different from that of the thermotropic smectic B solvents so far used by us, but the structural organization of the two phases can be strictly related. The thermotropic smectic mesophases have a layered structure and their constituting molecules have a fairly rigid core and flexible chains. This structure leads to an alternating sequence of rigid-core and alkyl chains sub-layers. This alternating sequence in a lyotropic lamellar phase may be identified in its polar and paraffinic sub-layers.

The disruptive effect of a solute molecule on a solvent structural organization and hence on its DSC profile is determined by the guest solubilization site. This disruptive effect is obviously less dramatic when the guest molecule is solubilized within the flexible alkyl chains, and profiles A- and C-like are thus expected. A B-like behavior may be due to solute intercalation within the rigid-core sub-layers. The more dramatic D-like deformation of the DSC profile is due to phase segregation process within the smectic bulk.

This approach provides a general frame for a structural interpretation of the DSC profiles of smectic solutions. The peak broadening at constant enthalpy (A-like case) may therefore be ascribed to an ASE localization within the liquid-like alkyl sublayers. But at the same time at least one shoulder ("3") appears (B-like case) and therefore some ASE is expected to be solubilized also within the rigid cores. At high ASE concentration, a D-like profile is displayed (peak "4") due to a new phase separation.

This interpretation perfectly matches the LD results[12] which provided our researches on the liquid crystalline catalysis with the way to a unifying structural picture, able to explain all the experimental data so far obtained from many different physical techniques[7-12]: this way was based on the evidence that ASE molecules are located in two different sites of the host smectic B structure, likely in the rigid core layer and in the region of the more flexible alkyl chains. Solute partition processes within smectic solvents were already suggested by ESR,[23] NMR[24–28] and fluorescence[29] measurements, but the LD spectra provided the clearest evidence of these equilibria by displaying a separate signal for each of the two sites.

The reactive site inside the core layers appears to be the more ordered and the far less populated. Probably, it is also the less reactive one: its crystal-like packing may prevent the molecular diffusion within the core-layers necessary for the encounters of the reagent molecules and for product formation.[24–27] The reactant jumping between the two sites is fast compared to the rate determining bimolecular process: the partition of the reactant molecules leads to a sort of pre-equilibrium-type situation with relative populations which are strongly dependent upon temperature and guest concentration.[12]

This (temperature-concentration)-dependent partition of solute between sites in rigid cores and in aliphatic tails can explain on one hand the quaternization rate depression for high initial MSE concentration[7,8] and on the other hand the remarkable upward curvature of the Arrhenius plot and the kinetic discontinuities observed within the smectic B phase in the case of ASE reaction.[12]

The x-ray diffraction profiles showed by mixtures of ZLI-1409 and ASE are basically the same as those of pure solvent (see Figure 4 and Table I). This may be due to the fact that guest perturbations of a very tight host molecular packing have a local, very short-range effect only. The smectic B structure, characterized by a well defined separation between the aliphatic and rigid core sub-layers is in fact mostly determined by the interactions among the cores. The tails contribute poorly to the overall packing energy but play a marked role by their flexibility[30] in absorbing and annihilating density defects and in dissolving non-mesomorphic solute molecules. The DSC band broadening by adding solute molecules is strongly determined by this ability of the chains. New shoulders or peaks are due to guest perturbation able to build up a new local structure with a new molecular correlation.

An evidence of the two sites location of ASE could be also obtained from the thermal dependence of the intermolecular distance (Table I). The higher values obtained at low solute concentration can be related to the penetration of ASE in the rigid cores sublayers at high temperature. On the other hand, at higher concentration the decreased transition temperature to the nematic phase and/or the presence of an eutectic do not allow this ASE jumping.

CONCLUSIONS

Smectic B solvents supply very anisotropic potentials to molecular orientations, as the solid phases can. But the looser packing of a smectic medium allows softer reactivity for the guest molecule. The high order and strong similarity of these mesophases to solid media make the steric requirements for a guest molecule solubilization very strict.

A detailed knowledge of the reactant–solvent mixture within the "reaction-pot" is strictly required to understand what is going on. This paper demonstrates the power of DSC to display a multisite distribution of the guest reactant molecule within solution.

References

1. M. J. S. Dewar and B. D. Mahlovsky, *J. Am. Chem. Soc.*, **96**, 460 (1974).
2. W. E. Bacon, *Pramana Suppl.*, **1**, 455 (1975) and references therein.
3. W. E. Bacon, Ling Kuo Jim and G. H. Brown, *Mol. Cryst. Liq. Cryst. (Lett.)*, **56**, 13 (1979).
4. W. E. Bacon, *J. Phys. (Paris)*, **36 C-1**, 409 (1975).
5. G. Aviv, J. Sagiv and A. Yogev, *Mol. Cryst. Liq. Cryst.*, **36**, 349 (1976).
6. G. Gottarelli and B. Samori, in "Liquid Crystals," S. Chandrasekhar Ed., Heiden & Sons, p. 505 (1980).
7. B. Samori and L. Fiocco, *J. Am. Chem. Soc.*, **104**, 2634 (1982).
8. P. De Maria, A. Lodi, B. Samori, F. Rustichelli and G. Torquati, *J. Am. Chem. Soc.*, **106**, 653 (1984).
9. G. Albertini, F. Rustichelli, G. Torquati, A. Lodi, B. Samori and G. Poeti, *Nuovo Cimento*, **2D**, 1327 (1983).
10. S. Melone, V. Mosini, R. Nicoletti, B. Samori and G. Torquati, *Mol. Cryst. Liq. Cryst.*, **98**, 399 (1983).
11. P. De Maria, P. Mariani, F. Rustichelli and B. Samori, *Mol. Cryst. Liq. Cryst.*, **116**, 115 (1984).
12. B. Samori, P. De Maria, P. Mariani, F. Rustichelli and P. Zani, *Tetrahedron*, **43**, 1409 (1987).
13. D. A. Hrovat, J. H. Liu, N. J. Turro and R. G. Weiss, *J. Am. Chem. Soc.*, **106**, 5291 (1984).
14. D. A. Hrovat, J. H. Liu, N. J. Turro and R. G. Weiss, *J. Am. Chem. Soc.*, **106**, 7033 (1984).
15. J. W. Leigh, *J. Am. Chem. Soc.*, **107**, 6114 (1985).
16. P. Mariani, B. Samori, A. S. Angeloni and P. Ferruti, *Liq. Cryst.*, **1**, 327 (1986).
17. L. Finzi, G. Maccagnani, S. Masiero, B. Samori and P. Zani, to be published.
18. E. Meirovitch, D. Igner, E. Igner, G. Moro and J. H. Freed, *J. Chem. Phys.*, **77**, 3915 (1982).
19. J. A. Leadbetter, Conf. Ser.-Inst. Phys. (Neutron Its Appl.), **64**, 277 (1983).
20. A. G. Lee, *Biochim. Biophys. Acta*, **413**, 11 (1975).
21. H. K. Jain and N. M. Wu, *J. Memb. Biology*, **34**, 157 (1977).
22. R. N. McElhaney, *Chem. Phys. Lipids*, **30**, 229 (1982).
23. E. Meirovitch and J. Freed, *J. Phys. Chem.*, **84**, 2459 (1980).
24. N. A. P. Vaz and J. W. Doane, *J. Chem. Phys.*, **79**, 2470 (1983).
25. E. Meirovitch and M. S. Broido, *J. Phys. Chem.*, **88**, 4316 (1983).

26. G. Moro, P. L. Nordio and U. Segre, *Chem. Phys. Lett.*, **105**, 440 (1984).
27. M. E. Moseley and A. Loewenstein, *Mol. Cryst. Liq. Cryst.*, **90**, 117 (1982).
28. L. S. Selwyn, R. R. Vold and R. L. Vold, *Mol. Phys.*, **55**, 287 (1985).
29. R. Subramanian, L. K. Patterson and H. Levanon, *Photochem. Photobiol.*, **41**, 511 (1985).
30. F. Barbarini, J. P. Chausse, C. Fabre, J. P. Germain, B. Deloche and J. Charvolin, *J. Phys. (Paris)*, **44**, 45 (1983).